User-centric Performance Optimization with Remote Radio Head Cooperation in C-RAN

Lei You and Di Yuan

Department of Information Technology, Uppsala University, Sweden
{lei.you; di.yuan}@it.uu.se

Abstract—In a cloud radio access network (C-RAN), distributed remote radio heads (RRHs) are coordinated by baseband units (BBUs) in the cloud. The centralization of signal processing provides flexibility for coordinated multi-point transmission (CoMP) of RRHs to cooperatively serve user equipments (UEs). We target enhancing UEs' capacity performance, by jointly optimizing the selection of RRHs for serving UEs, i.e., CoMP selection, and resource allocation. We analyze the computational complexity of the problem. Next, we prove that under fixed CoMP selection, the optimal resource allocation amounts to solving a so-called iterated function. Towards user-centric network optimization, we propose an algorithm for the joint optimization problem, aiming at scaling up the capacity maximally for any target UE group of interest. The proposed algorithm enables network-level performance evaluation for quality of experience.

Index Terms—Cloud radio access network; user-centric network; resource allocation; CoMP

I. Introduction

A. Background

CLOUD radio access network (C-RAN) enables virtualization of functionalities of base stations by centrally managing a "cloud" that is responsible for signal processing and coordination of geographically distributed remote radio heads (RRHs) [2]. The baseband units (BBUs) that are separately located in base stations under the traditional cellular network architecture, are centrally deployed in BBU pools in the cloud in the C-RAN architecture. The centralization of signal processing enables coordination among RRHs. This facilitates the implementation of coordinated multipoint transmission (CoMP) for improving spectrum efficiency [3]. The quality of service (QoS) may thus be enhanced by squeezing more out of the spectrum [2], [3].

For the upcoming 5G, the concept of *user-centric operation* [4]–[7] has been drawing attention recently. The paradigm of *user-centric C-RAN* targets enhancing the quality of experience (QoE), which looks outward from the end-user. Whether or not the performance benefits from utilizing more resource is up to the type of service in use. For example, video and audio streaming, email and file transfers, or VoIP, all have different levels of sensitivities to network QoS metrics (e.g. throughput, delay, or packet loss) that are influenced by resource allocation. Compared to allocating network resource purely subject to the QoS fairness [6], [8], [9], from the user-centric viewpoint, it is more rationale to allocate resource

based on user groups of different service types. In this context, *optimizing the capacity for a specific target group of UEs* becomes relevant.

Resource allocation in user-centric C-RAN faces more challenges compared to the traditional long-term evolution (LTE) cellular networks. First, as CoMP is assumed to be put in use by default under the C-RAN architecture, the network becomes more connected, resulting in more complex coupling relations between the network elements. The network performance is also affected by selecting the serving RRHs for user equipments (UEs), i.e., CoMP selection. Given this background, the paper targets jointly optimizing CoMP selection and resource allocation in order to increase the capacity for *any target group of users* in C-RAN.

B. Related Work

1) RRH selection and resource allocation: A number of studies have focused on optimizing CoMP or resource allocation in C-RANs. In [10], the authors studied CoMP-based interference mitigation in heterogeneous C-RANs. In [11], the authors investigated the joint transmission (JT) CoMP performance in C-RANs with large CoMP cluster size. The authors of [12] investigated resource allocation of CoMP transmission in C-RANs, and proposed a fairness-based scheme for enhancing the network coverage. In [13], the authors studied the joint cell-selection and resource allocation problem, in C-RANs without CoMP. In [14], a resource allocation problem was studied for C-RANs with a framework of small cells underlaying a macro cell. The study in [15] formulated an RRH selection optimization problem for power saving in C-RANs as a mixed integer linear programming model taking into account bandwidth allocation. A local search algorithm was proposed to solve the problem. In [16], the authors jointly optimized RRH selection and power allocation to minimize the total transmit power of the RRHs. The file caching status in RRHs is part of the setup. The problem was formulated in a non-convex form and solved by a Lagrange dual method. The authors of [17] investigated the weighted sum rate problem by jointly optimizing RRH selection and power allocation. By applying a Lagrange dual method, the authors derived an optimal solution to a special case where the number of sub-carrier is infinite. In [18], the authors studied the energy-aware utility maximization problem by jointly optimizing beamforming, BBU scheduling and RRH selection. The problem was decomposed and solved separately, yielding a heuristic solution. The authors of [19] formulated

an energy minimization problem with joint optimization of resource allocation and RRH selection. A greedy strategy was employed for RRH activation and pairing active RRHs to UEs. Under fixed RRH-UE association, the corresponding resource allocation was computed. The authors of [20] employed a statistical model for characterizing the traffic load of RRHs in C-RAN. The load incurred by UEs is directly related to the number of allocated resource blocks (RBs). A heuristic dynamic RRH assignment algorithm was proposed. The authors in [21]–[23] investigated the influence of RRH selection on the network resource usage efficiency and energy savings, while the dynamics and coupling between the resource consumption levels of RRHs are not taken into account.

2) QoS/QoE optimization in C-RAN: In [24], an abstract model of QoS-aware service-providing framework was proposed based on queueing theory. The model admits optimal solution obtained by convex optimization with respect to the service rate. In [5], the authors investigated joint precoding and RRH selection subject to QoS requirement of users. The joint optimization problem was decoupled into two stages (resulting in suboptimality), respectively for RRH selection and power minimization. The authors of [25] considered the single user case. A QoS-driven power- and rate-adaption scheme aiming at maximizing the user capacity was proposed. The authors showed the convexity of the formulation and solved it to the optimum with a Lagrange dual method. Reference [26] studied the problem of jointly optimizing RRH sleep control and transmission power over optical-fiber cables that connect RRHs to the cloud. The proposed network operation is based on a heuristic strategy aiming at minimizing the power consumption with guarantee of QoE. The QoE is defined to be the packet loss probability. In [27], the authors proposed a beamforming scheme to coordinate RRHs for improving QoE. The QoE is defined to be the weighted sum of sigmoidal QoS functions of users. The problem is to maximize the QoE subject to power constraints. A heuristic algorithm was proposed.

3) Resource allocation with load-coupling: A related line of research is the characterization of resource allocation in orthogonal-frequency-division multiple access (OFDMA) networks. A model that characterizes the coupling relationship of allocated resource among network entities is becoming adopted [1], [28]–[33]. By this model, a connection between network load and user bits demand in QoS/QoE satisfaction is established.

C. Motivation

One way of evaluating the performance with respect to QoS/QoE is to measure *how much of the user demand can be scaled up* before the network resource becomes exhausted. For fairness-based QoS enhancement, the problem was studied by computing the *maximum demand scaling factor* for all users [1], [32], [33], which is fundamentally based on computing the eigenvalue as well as the eigenvector for a non-linear system. References [1], [32], [33] employ a restricted setup of ours. Their solution approaches do not apply for our generalized scenario, as the resulting problem does not map to computing the eigenvalue and eigenvector anymore. Whether or not the

maximum capacity with respect to QoE-aware demand scaling can be effectively and efficiently computed remains open. Besides, under the C-RAN architecture, the interplay between network resource allocation and RRH cooperation needs to be captured. To the best of our knowledge, how to optimally perform *user-centric demand scaling* has not been addressed yet.

D. Contribution

The main contributions of this paper are summarized as follows. We propose a new framework for computing the *maximum demand scaling factor* for any given group of users in C-RAN. Our framework is a significant extension of the one used in [1], [32], [33]. Furthermore, based on this framework, we study the joint optimization problem of time-frequency resource allocation and CoMP selection, in terms of user-centric demand scaling. We address the tractability of this problem. To deal with the complexity, we propose an algorithm that alternates between CoMP selection and resource allocation. Specifically, we prove that, with fixed CoMP selection, the optimal resource allocation amounts to solving a so-called *iterated function*. Furthermore, we provide a partial optimality condition for improving CoMP selection and prove that it is naturally combined with our resource allocation method. The condition and the method are incorporated together to form our joint optimization algorithm. We remark that the solution method for demand scaling in [1], [32], [33] can only address a special case of ours. We further proved that, under fixed CoMP selection, our proposed method solves the resource allocation to global optimality. Finally, we show numerically how the joint optimization scheme can be used to scale up user demands for user-centric capacity enhancement. The obtained results reveal how CoMP improves the user capacity and how the user group size and the number of CoMP users affect the performance. To the best of our knowledge, this is the first paper that addresses user-centric demand scaling with load-coupling and CoMP.

E. Paper Organization

The paper is organized as follows. Section II gives the system model. Section III formulates the problem and analyzes its tractability. Section IV derives our solution method for problem solving. After discussing the numerical results in Section V, the paper is concluded in Section VI. The proofs of all theorems in Section IV are detailed in the Appendix. Throughout all sections, we use bold fonts to represent vectors/matrices, and capitalized letters in calligraphy to represent mathematical sets. As for function/mapping definitions, we use the notation $g : \text{var} \mapsto \text{expr}$ to represent a function/mapping $g(\text{var})$ with mathematical expression expr of variable var.

We use $\mathbb{R}_{++}$ to refer to all positive real numbers, i.e. $\mathbb{R}_{++} = (0, \infty)$. Similarly, we use $\mathbb{R}_+$ to refer to all non-negative real numbers, i.e. $\mathbb{R}_+ = [0, \infty)$.

II. SYSTEM MODEL

A. Notations

Denote by $\mathcal{R} = \{1, 2, \ldots, m\}$ the set of RRHs in a C-RAN. Denote by $\mathcal{J} = \{1, 2, \ldots, n\}$ the set of UEs. We use matrix

$\kappa \in \{0,1\}^{m \times n}$ to indicate the association between RRHs and UEs. The matrix κ is subject to optimization. For the sake of presentation, let us consider any given κ. For this κ, we use $\mathcal{R}_j$ and $\mathcal{J}_i$ as generic notations for the set of RRHs serving UE j and the set of UEs served by RRH i, respectively. Specifically, $i \in \mathcal{R}_j$ and $j \in \mathcal{J}_i$ if and only if $\kappa_{ij} = 1$. Note that κ characterizes CoMP selections, i.e., which UE is served by which RRHs. Single antenna case in C-RAN [34]–[36] is considered in this paper.

B. CoMP Transmission

Downlink is considered. Denote by p_i the transmit power of RRH i ($i \in \mathcal{R}$) on one resource block (RB). Denote by h_{ij} the channel gain between RRH i and UE j. Let x be the channel input symbol sent to UE j by the RRHs in $\mathcal{R}_j$. Entity x_k denotes the channel input symbol sent by the other RRHs that are not cooperatively serving UE j. The received channel output at UE j can be written as

$$s = \sum_{i \in \mathcal{R}_j} \sqrt{p_i} h_{ij} x + \sum_{k \in \mathcal{R} \setminus \mathcal{R}_j} \sqrt{p_k} h_{kj} x_k + \sigma_j. \qquad (1)$$

We assume that x and x_k ($k \in \mathcal{R} \setminus \mathcal{R}_j$) are independent zero-mean random variables of unit variance. Parameter σ_j models the noise of any user j. The signal-to-interference and noise ratio (SINR) of UE j is given below, by [37],

$$\gamma_j = \frac{|\sum_{i \in \mathcal{R}_j} \sqrt{p_i} h_{ij}|^2}{\sum_{k \in \mathcal{R} \setminus \mathcal{R}_j} w_{kj} + \sigma_j^2}, \qquad (2)$$

where w_{kj} is the interference received at UE j from RRH k. For any user, the interference it receives comes from those RRHs that are not serving the user, and the cooperative RRHs do not generate interference to the user [37]. We remark that the gains and noises can be different for users, and our solution method proposed later enables performance evaluation for scenarios with different user channel gains and noises.

C. Interference Modeling

We introduce the network-level interference model that is widely adopted in OFDMA systems, referred to as "*load-coupling*" [1], [28]–[33]. The model is shown to capture well the characterization of interference coupling [28]. Denote by M the total number of RBs in consideration. Define ρ_k as the proportion of allocated RBs of RRH k to serve all of its UEs. If $\rho_k = 0$, it means that there is no time-frequency resource in use by RRH k. In this case, k does not generate interference to others and $w_{kj} = 0$ ($j \in \mathcal{J} \setminus \mathcal{J}_k$). On the other hand, if $\rho_k = 1$, then all the RBs in RRH k are used for transmission and RRH k constantly interferes with others, i.e., $w_{kj} = p_k |h_{kj}|^2$ ($j \in \mathcal{J} \setminus \mathcal{J}_k$) [37]. For $0 < \rho_k < 1$, ρ_k serves as a scale parameter of interference:

$$w_{kj} = p_k |h_{kj}|^2 \rho_k. \qquad (3)$$

By the definition of ρ_k, it is referred to as *load of the RRH* k and can be intuitively explained as the likelihood that RRH k interferes with others. The network load vector is represented as $\boldsymbol{\rho} = [\rho_1, \rho_2, \ldots, \rho_m]$. Increasing any load ρ_k may lead to

the capacity enhancement of UEs in $\mathcal{J}_k$. On the other hand, as can be seen from (3), the increase of ρ_k results in higher interference from k to other UEs $\mathcal{J} \setminus \mathcal{J}_k$, which may cause the load levels of RRHs other than k to increase. Note that a heavily loaded RRH interferes more severely to others, while an RRH that is slightly loaded tends not to generate much interference.

D. User Demand Scaling

Denote by B the bandwidth per RB. The achievable bit rate for UE j by the transmissions of j's serving RRHs is denoted by a function $C_j : \mathbb{R}_+^n \to \mathbb{R}_+$ of SINR, which in turn is a function of the network load $\boldsymbol{\rho}$:

$$C_j : \boldsymbol{\rho} \mapsto MB \log_2(1 + \gamma_j(\boldsymbol{\rho})). \qquad (4)$$

Denote by d_j the bits demand of UE j ($j \in \mathcal{J}$). Given the proportion of allocated RBs in RRHs that are not serving UE j, the expression $\frac{d_j}{C_j(\boldsymbol{\rho})}$ gives the proportion of required RBs for the RRHs serving UE j to satisfy this demand d_j. We remark that $C_j(\boldsymbol{\rho})$ is non-linear of the proportion of allocated RBs in the interfering RRHs. Let μ_j represent the proportion of RBs allocated to j by j's serving RRHs. As for all UEs in $\mathcal{J}$, we let $\boldsymbol{\mu} = [\mu_1, \mu_2, \ldots, \mu_n]$. Because of CoMP, the RBs used by all these RRHs for serving j are the same. For allocating sufficient proportion of RBs to satisfy UE j's demand, we have:

$$\mu_j \geqslant \frac{d_j}{C_j(\boldsymbol{\rho})}. \qquad (5)$$

By the definition of ρ_i ($i \in \mathcal{R}$), we have

$$\rho_i = \sum_{j \in \mathcal{J}_i} \mu_j. \qquad (6)$$

Denote by $\bar{\rho}$ the load limit of RRHs. Then we need to keep $\rho_i \leqslant \bar{\rho}$ ($i \in \mathcal{R}$), otherwise the network is overloaded, meaning that the available resource is not sufficient for delivering the demands. Combining (4) with (6), for any $j \in \mathcal{J}$, we use $f_j : \mathbb{R}_+^n \mapsto \mathbb{R}_{++}$ to denote the following function:

$$f_j : \boldsymbol{\mu} \mapsto \frac{d_j}{C_j(\boldsymbol{\mu})}. \qquad (7)$$

Given $\mathbf{d} = [d_1, d_2, \ldots, d_n]$, consider for QoE of a specific UE j, we would like to scale up d_j by a *demand scaling factor* α ($\alpha > 0$). The reason of considering the maximization of α is it tells how much traffic growth the network can accommodate by optimizing user association, as such it provides information related to network capacity. With demand scaling, μ_j needs to satisfy:

$$\mu_j \geqslant \alpha f_j(\boldsymbol{\mu}). \qquad (8)$$

Due to the mutual coupling relationship of the elements in the vector $\boldsymbol{\mu}$, scaling up the demand for UE j may cause the increase of the interference to others such that the bits demand of other UEs cannot be satisfied. Therefore, one should also make sure that the following equation holds:

$$\boldsymbol{\mu}_{-j} \geqslant \mathbf{f}_{-j}(\boldsymbol{\mu}). \qquad (9)$$

where $\boldsymbol{\mu}_{-j}$ and $\mathbf{f}_{-j}$ ($j \in \mathcal{J}$) represent the vectors without the j_{th} element. Finally, the resource limits are subject to the inequalities $\sum_{j \in \mathcal{J}_i} \mu_j \leqslant \bar{\rho}$ ($i \in \mathcal{R}$). More generally, one can scale up the demand for any UE group $\mathcal{S}$ ($\mathcal{S} \subseteq \mathcal{J}$). One way to view $\mathcal{S}$ is the set of users with elastic traffic. For the other users in $\mathcal{J} \setminus \mathcal{S}$, their demand has to be satisfied without any scaling. For the special case of $\mathcal{S} = \mathcal{J}$, maximum demand scaling corresponds to finding out how much traffic growth is possible before the resource is exhausted.

Note that (8) and (9) form a system of non-linear inequalities in terms of $\boldsymbol{\mu}$ and α, which cannot be readily solved. There is a special case that is however easy. With $\mathcal{S} = \mathcal{J}$, one can write (8) and (9) as $\boldsymbol{\mu} \geqslant \alpha \mathbf{f}(\boldsymbol{\mu})$, i.e., the demand scaling is on all the UEs. To use the minimum amount of resource to satisfy the demands, we have $\frac{1}{\alpha}\boldsymbol{\mu} = \mathbf{f}(\boldsymbol{\mu})$. In this case, $\frac{1}{\alpha}$ and $\boldsymbol{\mu}$ are exactly the eigenvalue and eigenvector of this non-linear equations system and can be solved by the concave Perron-Frobenius Theorem [38]. However, the conclusion does not hold for the general case $\mathcal{S} \subseteq \mathcal{J}$. Indeed, the general case is fundamentally different, as α is not the scaling parameter in each dimension of the function $\mathbf{f}$ when $\mathcal{S} \subset \mathcal{J}$.

III. PROBLEM FORMULATION AND COMPLEXITY ANALYSIS

In this section, we formulate the demand scaling problem and prove its computational complexity. Recall that $\mathcal{R}_j$ and $\mathcal{J}_i$ characterize the CoMP selection and are induced by the matrix $\boldsymbol{\kappa}$. To characterize CoMP selection, we treat $\mathcal{R}_j$ ($j \in \mathcal{J}$) and $\mathcal{J}_i$ ($i \in \mathcal{R}$) as mappings shown below, which map any matrix $\boldsymbol{\kappa}$ to the sets of serving RRHs and served UEs, respectively.

$$\mathcal{R}_j : \boldsymbol{\kappa} \mapsto \{i | \kappa_{ij} = 1\} \tag{10}$$

$$\mathcal{J}_i : \boldsymbol{\kappa} \mapsto \{j | \kappa_{ij} = 1\} \tag{11}$$

The problem is formulated in (12). Solving (12) is equivalent to solving the maximization of throughput satisfaction ratio for $\mathcal{S}$ subject to the max-min fairness[1] [32].

$$[\textit{MaxD}] \quad \max_{\alpha > 0, \boldsymbol{\mu} \geqslant 0, \boldsymbol{\kappa}} \alpha \tag{12a}$$

$$\text{s.t.} \quad \mu_j \geqslant \alpha f_j(\boldsymbol{\mu}, \boldsymbol{\kappa}) \quad j \in \mathcal{S} \tag{12b}$$

$$\mu_j \geqslant f_j(\boldsymbol{\mu}, \boldsymbol{\kappa}) \quad j \in \mathcal{J} \setminus \mathcal{S} \tag{12c}$$

$$\sum_{j \in \mathcal{J}_i} \mu_j \leqslant \bar{\rho} \quad i \in \mathcal{R} \tag{12d}$$

$$\kappa_{ij} \in \{0, 1\} \quad i \in \mathcal{R}, \ j \in \mathcal{J} \tag{12e}$$

The objective is to maximize the demand scaling factor α for a given set of UEs $\mathcal{S}$ ($\mathcal{S} \subseteq \mathcal{J}$), given the base user demand $\mathbf{d}$ ($\mathbf{d}$ is in the expression of the function f_j). Remark that the function $f_j(\boldsymbol{\mu})$, defined in (7), computes

[1]We remark that (12b) can be equivalently re-written as $\alpha \leqslant \min_{j \in \mathcal{S}} \mu_j C_j(\boldsymbol{\rho}, \boldsymbol{\kappa})/d_j$. Then (12) can be reformulated as

$$\max_{\boldsymbol{\mu} \geqslant 0, \boldsymbol{\kappa}} \min_{j \in \mathcal{S}} \frac{\mu_j C_j(\boldsymbol{\rho}, \boldsymbol{\kappa})}{d_j} \text{ s.t. (12c)–(12e)}$$

which is exactly the maximization problem for user-specific throughput satisfaction ratio. The demand d_j is satisfiable if and only if this ratio is greater than or equal to one.

the minimum required proportion of resource for satisfying the demand d_j of UE j, and μ_j is the resource allocated to UE j. Therefore constraints (12c) ensure that sufficient time-frequency resources are allocated for satisfying the demands d_j ($j \in \mathcal{J} \setminus \mathcal{S}$). The UEs in $\mathcal{S}$ can be regarded as being throughput-oriented such that delivering more demands leads to higher satisfaction, as imposed by constraints (12b). Hence, the objective is maximizing the demand scaling factor α for $\mathcal{S}$. Constraint (12d) imposes the maximum RRH load limit. The variable matrix $\boldsymbol{\kappa}$ controls the CoMP selection.

Solving (12) yields an a network-level evaluation for user group data rate enhancement [28]–[33], with the channel coefficients and noises corresponding to approximate averages upon the time scale of interest of load coupling. This type of modeling is commonly used for studies and analysis at a macroscopic level, and in fact variations of gains and noises have little impact on the accuracy of the load coupling model [28]. In addition, we remark that the demand scaling factor is the satisfaction ratio of the user demands in $\mathcal{S}$. That is, given base demands d_j ($j \in \mathcal{J}$) and the RRH resource limit $\bar{\rho}$, the solution α^* obtained by solving *MaxD* is indeed the maximum satisfiable ratio of d_j ($j \in \mathcal{S}$) within the resource limit. Namely, if d_j ($j \in \mathcal{S}$) are satisfiable, then we have $\alpha^* \geqslant 1$. Otherwise $\alpha^* < 1$ holds and α^* is the satisfiable proportion of the demands d_j ($j \in \mathcal{S}$).

We remark that, the method of scaling the demand for $\mathcal{J}$, which is a special case of *MaxD*, does not generalize to priority-aware resource optimization.

Theorem 1 below shows the $\mathcal{NP}$-hardness of *MaxD*. The basic idea behind the proof is to show that there is one scenario that is at least as hard as *3-SAT*.

Theorem 1. *MaxD is $\mathcal{NP}$-hard.*

Proof. We prove the theorem by a polynomial-time reduction from the 3-satisfiability (*3-SAT*) problem that is $\mathcal{NP}$-complete. Consider a *3-SAT* problem with N_1 Boolean variables $b_1, b_2, \ldots, b_{N_1}$, and N_2 clauses. A Boolean variable or its negation is referred to as a literal, e.g. $\hat{b}_i$ is the negation of b_i. A clause is composed by a disjunction of exactly three distinct literals, e.g., $(b_1 \vee b_2 \vee \hat{b}_3)$. The *3-SAT* problem amounts to determining whether or not there exists an assignment of true/false to the variables, such that all clauses are satisfied.

The corresponding feasibility problem of *MaxD* is that whether or not there exists any $(\alpha, \boldsymbol{\mu}, \boldsymbol{\kappa})$ such that constraints (12a)–(12e) are satisfied. To make the reduction, we construct a specific network scenario as follows. Suppose we have $N_1 + N_2 + 1$ UEs in total, denoted by $v_0, v_1, v_2, \ldots, v_{N_1+N_2}$, respectively. Also, we have in total $2N_1 + N_2 + 1$ RRHs, denoted by $a_1, \hat{a}_1, a_2, \hat{a}_2, \ldots, a_{N_1}, \hat{a}_{N_1}$, and $a_0, a_{N_1+1}, \ldots, a_{N_1+N_2}$. The RRHs $a_1, \hat{a}_1, a_2, \hat{a}_2, \ldots, a_{N_1}, \hat{a}_{N_1}$ are the counter parts to the $2N_1$ variables and their negations. And the RRHs $a_{N_1+1}, \ldots, a_{N_1+N_2}$ are corresponding to the N_2 clauses. For each v_i ($1 \leqslant i \leqslant N_1$), we set $\{a_i, \hat{a}_i\}$ as its candidate RRHs. For v_0 and each v_j ($N_1 < j \leqslant N_1 + N_2$), we have exactly one candidate RRHs. Therefore, their serving RRHs are fixed, i.e., $\mathcal{R}_{v_0} = \{a_0\}$ and $\mathcal{R}_{v_j} = \{a_j\}$. Let

$p_{a_0} = 3N_1 + 1$. For $1 \leqslant i \leqslant N_1$, let $p_{a_i} = p_{\hat{a}_i} = 3.0$. For $N_1 < j \leqslant N_1 + N_2$, let $p_{a_j} = 3.0$. For UE v_0, $|h_{a_0,v_0}|^2 = |h_{a_i,v_0}|^2 = |h_{\hat{a}_i,v_0}| = 1.0$ ($1 \leqslant i \leqslant N_1$). For any UE v_i ($1 \leqslant i \leqslant N_1$), $|h_{a_i,v_i}|^2 = |h_{\hat{a}_i,v_i}|^2 = 1.0$. For any UE v_j ($N_1 < j \leqslant N_1 + N_2$), $|h_{a_i,v_j}|^2$ and $|h_{\hat{a}_i,v_j}|^2$ ($1 \leqslant i \leqslant N_1$) equal $\frac{1}{3}$ if b_i and $\hat{b}_i$ appears in clause j, respectively. In addition, $|h_{a_j,v_j}|^2 = 1.0$ ($N_1 < j \leqslant N_1 + N_2$). The gain values between all other RRH-UE pairs are negligible, treated as zero. The noise power σ_j^2 ($\forall j \in \mathcal{J}$) is 1.0. We normalize the demands of UEs by $B \times M$, such that $d_{v_i} = 2.0$ ($1 \leqslant i \leqslant N_1$) and $d_{v_0} = d_{v_j} = 1.0$ ($N_1 < j \leqslant N_1 + N_2$). Below we establish connections between solutions of *MaxD* and those of *3-SAT*. For *MaxD*, note that if $(1, \mu, \kappa)$ is not feasible, then (α, μ, κ) with $\alpha > 1$ is not either.

First, we note that each UE j ($0 \leqslant j \leqslant N_1 + N_2 + 1$) should be served by at least one RRH, otherwise C_j equals 0 and constraint (12b) or (12c) would be violated. Thus, a_0 is serving v_0 and $a_{N_1+1}, a_{N_1+2}, \ldots, a_{N_1+N_2}$ are serving $v_{N_1+1}, v_{N_1+2}, \ldots, v_{N_1+N_2}$, respectively. Second, it can be verified that v_i ($1 \leqslant i \leqslant N_1$) can only be served by exactly one RRH in $\{a_i, \hat{a}_i\}$, i.e., either $\mathcal{R}_{v_i} = \{a_i\}$ or $\mathcal{R}_{v_i} = \{\hat{a}_i\}$. This is because, for $1 \leqslant i \leqslant N_1$, the interference w_{a_i,v_0} (or $w_{\hat{a}_i,v_0}$) generated from each a_i (or $\hat{a}_i$) to v_0 is 3.0, if exactly one of $\{a_i, \hat{a}_i\}$ serves v_i: We assume a_i serves v_i, then

$$w_{a_i,v_0} = p_{a_i}|h_{a_i,v_0}|^2 \rho_{a_i} = 3.0 \times \frac{2.0}{\log_2(1 + |\sqrt{3}|^2)} = 3.0$$

In this case, one can verify that a_0 is fully loaded. In addition, letting any v_i ($1 \leqslant i \leqslant N_1$) served by both a_i and $\hat{a}_i$ results an interference to v_0 being larger than 3.0, i.e.

$$w_{a_i,v_0} + w_{\hat{a}_i,v_0} = 6.0 \times \frac{2.0}{\log_2(1 + |2\sqrt{3}|^2)} > 3.0$$

Then a_0 would be overloaded ($\rho_{a_0} > 1$). Besides, for each clause j ($N_1 < j \leqslant N_2$), the three corresponding RRHs cannot be all active in serving UEs. Otherwise, the RRH that is serving the UE corresponding to this clause would be overloaded. To see this, consider a clause $(b_1 \vee b_2 \vee \hat{b}_3)$ and its corresponding RRHs a_1, a_2 and $\hat{a}_3$. Assume this clause is associated with some UE j ($N_1 < j \leqslant N_1 + N_2$). By the above discussion, any of a_1, a_2 and $\hat{a}_3$ is fully loaded if it is active. Then, if all of them are active, we have

$$w_{a_1,v_j} = w_{a_2,v_j} = w_{\hat{a}_3,v_j} = 3.0 \times \frac{1}{3} \times 1.0 = 1.0$$

and thus for this UE j ($N_1 < j \leqslant N_1 + N_2$) we have

$$\rho_{a_j} = \frac{d_{v_j}}{\log_2\left(1 + \frac{p_{a_j}|h_{a_j,v_j}|^2}{w_{a_1,v_j} + w_{a_2,v_j} + w_{\hat{a}_3,v_j} + \sigma_{v_j}^2}\right)}$$
$$= \frac{1.0}{\log_2\left(1 + \frac{3.0 \times 1.0}{3.0 \times 1.0 + 1.0}\right)} > 1.0$$

On the other hand, one can verify that if less than three of a_1, a_2 and $\hat{a}_3$ are active for serving UEs, then $\rho_{a_j} \leqslant 1$.

Now suppose there is an RRH-UE association that is feasible. For each Boolean variable b_i, we set b_i to be true if $\hat{a}_i$ is serving UE v_i. Otherwise, v_i must be served by a_i

and we set b_i to false. Now we evaluate the satisfiability of each clause. For the sake of presentation, denote this clause by $(b_1 \vee b_2 \vee \hat{b}_3)$ as an example. The clause is satisfied if and only if at least one of its literals being true. As discussed above, a feasible solution for the constructed instance of *MaxD* cannot have all the three corresponding RRHs a_1, a_2, and $\hat{a}_3$ being in the status of serving UEs. Therefore, at least one of a_1, a_2, and $\hat{a}_3$ should be idle, meaning that the corresponding one of b_1, b_2, or $\hat{b}_3$ is set to be true. Therefore, based a feasible solution of the constructed problem, a feasible solution of the *3-SAT* problem instance can be accordingly constructed. Conversely, suppose we have a feasible solution for a *3-SAT* instance. Then we choose a_i to serve v_i if $\hat{b}_i$ is true, otherwise $\hat{a}_i$ is selected instead. Doing so satisfies all the demands for UEs j ($0 \leqslant j \leqslant N_1$). Furthermore, the demands of UEs i ($N_1 < i \leqslant N_1 + N_2$) are satisfied as well, since at most two out of the three RRHs defined for the three literals of the clause will be serving UE. Thus the RRH-UE association is feasible for the constructed instance of *MaxD*. Hence the conclusion. $\square$

Since *MaxD* is $\mathcal{NP}$-hard, one cannot expect any exact algorithm with good scalability for solving *MaxD* optimally, unless $\mathcal{P} = \mathcal{NP}$.

IV. PROBLEM SOLVING

In this section, we derive theoretical foundations for an algorithm solving *MaxD*. We introduce some basic mathematical concepts in Section IV-A. In Section IV-B we solve *MaxD* to global optimum *under fixed CoMP selection*, which serves as a sub-routine for the overall algorithm. In Section IV-C we give a partial optimality condition for optimizing the CoMP selection. An algorithm that alternates between CoMP selection and resource allocation is proposed in Section IV-D. We further show that considering the case $\mathcal{S} \subseteq \mathcal{J}$ enables to optimize per-user rate based on the user's priority, which enables gauging the network performance enhancement in a finer granularity in Section IV-E. The services with elastic demands could be put into the group $\mathcal{S}$ for QoS enhancement, while keeping the demands of other inelastic services being strictly satisfied. In Section IV-F, we give a computationally efficient bounding scheme that yields upper bound for *MaxD* under two extra constraints.

A. Basics

The following lemma shows a property of the function $\mathbf{f}(\mu)$. The result follows the reference [30, Lemma 6].

Lemma 2. *Function $\mathbf{f}(\mu)$ is a standard interference function (SIF) [39] for non-negative μ, i.e. the following properties hold:*
1) $\mathbf{f}(\mu') \geqslant \mathbf{f}(\mu)$ *if $\mu' \geqslant \mu$.*
2) $\beta\mathbf{f}(\mu) > \mathbf{f}(\beta\mu)$ ($\beta > 1$).

The main property of an SIF is that a fixed point, if exists, is unique and can be computed via fixed-point iterations. To be more specific, a vector μ satisfying $\mu = \mathbf{f}(\mu)$, if exists, is unique and can be obtained by the iterations $\mu^{(k)} = \mathbf{f}(\mu^{(k-1)})$ ($k \geqslant 1$) with any $\mu^{(0)} \in \mathbb{R}_+^n$.

B. Computing the Optimum for Given CoMP Selection

In this subsection, we show that solving *MaxD* with fixed CoMP selection amounts to solving an iterated function. In mathematics, an iterated function is a function from some set to the set itself. Solving an iterated function lies on finding a fixed point of it. The problem is formulated in (13) below, in which $\mathcal{R}_j$ ($j \in \mathcal{J}$) and $\mathcal{J}_i$ ($i \in \mathcal{R}$) are given. The problem in (13) is exactly *MaxD* under fixed CoMP selection κ.

$$\max_{\alpha > 0, \mu \geqslant 0} \quad \alpha \tag{13a}$$

$$\text{s.t.} \quad \mu_j \geqslant \alpha f_j(\mu) \quad j \in \mathcal{S} \tag{13b}$$

$$\mu_j \geqslant f_j(\mu) \quad j \in \mathcal{J} \backslash \mathcal{S} \tag{13c}$$

$$\sum_{j \in \mathcal{J}_i} \mu_j \leqslant \bar{\rho} \quad i \in \mathcal{R} \tag{13d}$$

The problem in (13) is a subproblem of *MaxD*. The motivation of deriving such a subproblem is based on the conclusion in Lemma 2 that the function $f(\mu, \kappa)$ under fixed κ is an SIF in μ. Below we derive a solution method for achieving global optimum of (13) based on the foundational properties of SIF, which justifies our decomposition approach. For the sake of presentation, for any μ, we denote by H a function that gives the normalized maximum load, i.e.,

$$H : \mu \mapsto \frac{1}{\bar{\rho}} \max_{i \in \mathcal{R}} \sum_{j \in \mathcal{J}_i} \mu_j. \tag{14}$$

Before presenting the solution method for (13), we outline two lemmas for optimality characterization. The two lemmas enable a reformulation that can be solved by an iterated function.

Lemma 3. $[\alpha^*, \mu^*]$ *is optimal to* (13) *only if* $H(\mu^*) = 1$ *and* $\mu_j^* = \alpha f_j(\mu^*)$ *for some* $j \in \mathcal{S}$.

Proof. Suppose $[\alpha^*, \mu^*]$ is an optimal solution such that all inequalities strictly hold in (13b). Then one can increase α^* to $\alpha' = \alpha^* + \epsilon$. By setting ϵ to be a sufficiently small positive value, one can obtain a feasible solution $[\alpha', \mu^*]$ with objective value α', which conflicts the assumption that $[\alpha^*, \mu^*]$ is optimal. Therefore, there exists some j ($j \in \mathcal{S}$) such that $\mu_j^* = \alpha f_j(\mu^*)$.

Obviously any solution $[\alpha^*, \mu^*]$ with $H(\mu^*) > 1$ is infeasible because at least one of (13d) is violated. Now suppose $H(\mu^*) < 1$. Then we increase μ^* to $\mu' = \beta \mu^*$ ($\beta = 1 + \epsilon$, $\epsilon > 0$). With ϵ being sufficiently small, μ' satisfies (13d). Due to the scalability of $f(\mu)$, we have

$$f(\beta \mu^*) < \beta f(\mu^*). \tag{15}$$

Consider (13b) for μ^*, which reads for any $j \in \mathcal{S}$

$$\mu_j^* \geqslant \alpha f_j(\mu^*) \Leftrightarrow \beta \mu_j^* \geqslant \alpha \beta f_j(\mu^*) \tag{16}$$

Combining (15) with (16) we have

$$\beta \mu_j^* > \alpha f_j(\beta \mu^*) \Leftrightarrow \mu_j' > \alpha f_j(\mu'). \tag{17}$$

The same process applies for deriving $\mu_j > f_j(\mu')$ for $j \in \mathcal{J} \backslash \mathcal{S}$. Therefore, μ' is a feasible solution to (13) such that all inequalities in (13b) and (13c) strictly hold. Under μ', one can increase α^* to α' as earlier in the proof, to obtain a better objective value, which conflicts with our assumption that $[\alpha^*, \mu^*]$ is optimal.

Thus, at the optimum of *MaxD* there is at least one UE j ($j \in \mathcal{S}$) such that $\mu_j^* = \alpha^* f_j(\mu^*)$ with $H(\mu^*) = 1$. $\qquad \square$

By Lemma 3 we know that a solution is optimal to (13) only if there exists a fully loaded RRH. Intuitively, if all RRHs in the C-RAN have unused time-frequency resource, then one can improve the objective function such that more bits would be delivered to UEs.

Lemma 4. $[\alpha^*, \mu^*]$ *is optimal to* (13) *if* (13b) *and* (13c) *all hold as equality and* $H(\mu^*) = 1$.

Proof. Suppose (13b) and (13c) hold for all $j \in \mathcal{J}$ as equalities with $[\alpha^*, \mu^*]$. Consider any α' ($\alpha' > \alpha^*$). Replacing α^* by α' in (13b) causes (13b) being violated. Thus μ_j^* ($j \in \mathcal{S}$) must increase to have (26b) remains satisfied. Then $f(\mu)$ would grow due to its monotonicity, resulting in the violations of (13c). Therefore, to have (13b) and (13c) remain satisfied, the vector μ must be increased. Denote by μ' the newly obtained resource allocation. Since $H(\mu^*) = 1$, then we must have $H(\mu') > 1$ which violates some constraint in (13d). Hence the conclusion. $\qquad \square$

Next we derive a solution method that achieves the global optimum of (13). We define function F_α as follows.

$$F_\alpha : \mu \mapsto \left[\frac{f_1(\mu)}{\pi_1(\alpha)}, \frac{f_2(\mu)}{\pi_2(\alpha)}, \dots, \frac{f_n(\mu)}{\pi_n(\alpha)} \right] \tag{18}$$

where

$$\pi_j(\alpha) = \begin{cases} 1 & j \in \mathcal{S} \\ \alpha & \text{otherwise} \end{cases} \tag{19}$$

Note that for any given $\alpha > 0$, the function F_α is an SIF in μ. The problem in (13) can be reformulated below.

$$\max_{\alpha \geqslant 1, \mu \geqslant 0} \alpha \text{ s.t. } \alpha F_\alpha(\mu) \leqslant \mu, H(\mu) = 1. \tag{20}$$

The recursive equations in Theorem 5 below give the solution method for solving (20) (and equivalently (13)). The optimality of this method is guaranteed by Theorem 6. The proofs of both Theorem 5 and Theorem 6 are in the Appendix. The symbol "$\circ$" denotes the function composition, i.e. $g_1 \circ g_2(\text{var}) = g_1(g_2(\text{var}))$.

Theorem 5. *Denote* $[\alpha^*, \mu^*] = \lim_{k \to \infty} [\alpha^{(k)}, \mu^{(k)}]$, *where*

$$\alpha^{(k)} = \frac{1}{H \circ F_{\alpha^{(k-1)}}(\mu^{(k-1)})}, \ k \geqslant 1 \tag{21}$$

and

$$\mu^{(k)} = \frac{F_{\alpha^{(k-1)}}(\mu^{(k-1)})}{H \circ F_{\alpha^{(k-1)}}(\mu^{(k-1)})}, \ k \geqslant 1, \tag{22}$$

with $\alpha^{(0)} > 0$ *and* $\mu^{(0)} \in \mathbb{R}_+^n$. *Then* $H(\mu^*) = 1$ *holds.*

Theorem 6. $[\alpha^*, \mu^*]$ *in Theorem 5 is optimal to* (13).

Theorem 5 and Theorem 6 guarantee that for an arbitrary set of UEs $\mathcal{S}$ in the network, one can iteratively compute the maximum demand scaling factor α^* for $\mathcal{S}$. As a special case, when $\pi_j(\alpha) = 1$ for all $j \in \mathcal{J}$, solving the problem in (20)

is to find the eigenvalue μ and the eigenvector $1/\alpha$ of the equation system $f(\mu) = (1/\alpha)\mu$ such that $H(\mu) = 1$. The iterative solution method in Theorem 5 serves as a subroutine for solving *MaxD*, shown in Section IV-D later.

C. CoMP Selection Optimization

We show a lemma for optimizing the CoMP selection. The detailed proof of the lemma is based on [40, Theorem 3]. The following notations are introduced. We consider two matrices κ and κ' with the following relationship: Each column in κ has at least one non-zero element (meaning that every UE is associated to at least one RRH); There exists exactly one RRH-UE pair (i, j) such that $\kappa_{ij} = 0$ and $\kappa'_{ij} = 1$, respectively; For any other pair (r, q), $\kappa'_{rq} = \kappa_{rq}$. Note that the only difference between the two associations κ and κ' is that κ' includes the CoMP link from RRH i to UE j while κ does not. Denote by μ^* and μ'^* the corresponding optimal resource allocations obtained respectively by κ and κ' (i.e. $\mu^* = F_\alpha(\mu^*, \kappa)$ and $\mu'^* = F_\alpha(\mu'^*, \kappa')$). For the sake of presentation, given some α ($\alpha > 0$), we represent ρ_i as a function of the resource allocation μ and the RRH-UE association κ:

$$\rho_i : [\mu, \kappa] \mapsto \sum_{j \in \mathcal{J}_i(\kappa)} F_{\alpha,j}(\mu, \kappa). \qquad (23)$$

Consider two sequences $\mu^{(0)}, \mu^{(1)}, \ldots, \mu^{(\infty)}$ and $\rho^{(0)}, \rho^{(1)}, \ldots, \rho^{(\infty)}$, where $\mu^{(k)} = f(\rho^{(k-1)}, \kappa')$, $\rho^{(k)} = \rho(\mu^{(k-1)}, \kappa)$ for $k \geqslant 1$, with $\mu^{(0)} = \mu^*$ and $\rho^{(0)} = \rho(\mu^{(0)}, \kappa)$. The convergence of the two sequences is guaranteed as the function F_α with fixed α is an SIF in both μ and ρ [40]. We provide the following lemma.

Lemma 7. $\rho(\mu'^*, \kappa') \leqslant \rho(\mu^*, \kappa)$ *if for any* $k \geqslant 1$ *we have* $\rho_i(\mu^{(k)}, \kappa') \leqslant \rho_i^{(k)}$.

Lemma 7 serves as a sufficient condition for RRH load improvement by CoMP. Specifically, in order to check whether adding a CoMP link between RRH i and UE j would reduce the load levels of RRHs, we iteratively construct the two sequences $\mu^{(0)}, \mu^{(1)}, \ldots, \mu^{(\infty)}$ and $\rho^{(0)}, \rho^{(1)}, \ldots, \rho^{(\infty)}$. Once there exists $k \geqslant 1$ such that $\rho_i(\mu^{(k)}, \kappa') \leqslant \rho_i^{(k)}$, we conclude that the bits demand by all UEs can be satisfied with lower time-frequency resource consumption (i.e. the load of RRH) under the association κ' than κ. In Section IV-D below, we show that the condition in Lemma 7 can be incorporated with the solution method in Theorem 5, to form our joint optimization algorithm.

D. Algorithm

The theoretical properties derived in Section IV-B and Section IV-C enable an algorithm for *MaxD*. To be more specific, given any RRH-UE association κ, one can obtain the corresponding maximum scaling factor α^* together with μ^* iteratively by (21) and (22) in Theorem 5. At the convergence, $H(\mu^*) = 1$ holds by Theorem 5. Taking one step further, if we fix α^* and consider all the candidate RRHs for each UE, using Lemma 7 (in Section IV-C) enables us to determine whether a new association κ' that includes some newly added CoMP

link would lead to load improvement. If yes, the corresponding resource allocation μ' under κ' must have $H(\mu') < 1$. Then by Lemma 3, the current solution $[\alpha^*, \mu']$ is not optimal. Once the load is improved, applying (21) and (22) under κ' again guarantees an overall improvement. We remark that Algorithm 1 works in an online manner in terms of the candidate RRH-UE pairs. To be specific, in each iteration of the outer loop, once a new CoMP link is added, the demand scaling factor α is guaranteed to be increased by the end of this iteration, based on the discussion above. This process is detailed in Algorithm 1.

Algorithm 1: Joint Demand Scaling and CoMP Selection

Input: $\kappa^{(0)}, \mathcal{S}, \epsilon > 0, \bar{\rho}$
Output: $\kappa^*, \mu^*, \alpha^*$
1   $\alpha^{(0)} \leftarrow 1$; (Or other positive number)
2   $\mu^{(0)} \leftarrow 0$; (Or other non-negative vector)
3   **repeat**
4   **for** $i \leftarrow 1$ to m, $j \leftarrow 1$ to n, with $\kappa_{ij}^{(c)} = 0$ **do**
5       $k \leftarrow 1$;
6   **repeat**
7         $\kappa^{(c)} \leftarrow \kappa^{(c-1)}$;
8         $\kappa' \leftarrow \kappa^{(c)}$;
9         $\kappa'_{ij} \leftarrow 1$;
10        $\rho^{(k)} \leftarrow \rho(\mu^{(k-1)}, \kappa^{(c)})$;
11        $\mu^{(k)} \leftarrow F_\alpha(\rho^{(k)}, \kappa')$;
12   **if** $\rho_i(\mu^{(k)}, \kappa') \leqslant \rho_i^{(k)}$ **then**
13          $\kappa^{(c)} \leftarrow \kappa'$;
14        $k \leftarrow k + 1$;
15   **until** $\|\mu^{(k)} - \mu^{(k-1)}\| < \epsilon$;
16       $h \leftarrow 1$;
17   **repeat**
18         $\alpha^{(h)} \leftarrow \frac{1}{H \circ F_{\alpha^{(h-1)}}(\mu^{(h-1)}, \kappa^{(c)})}$;
19         $\mu^{(h)} \leftarrow \frac{F_{\alpha^{(h-1)}}(\mu^{(h-1)}, \kappa^{(c)})}{H \circ F_{\alpha^{(h-1)}}(\mu^{(h-1)}, \kappa^{(c)})}$;
20         $h \leftarrow h + 1$;
21   **until** $\|[\alpha^{(h)}, \mu^{(h)}] - [\alpha^{(h-1)}, \mu^{(h-1)}]\| < \epsilon$;
22       $\alpha \leftarrow \alpha^{(h)}$;
23       $\mu \leftarrow \mu^{(h)}$;
24     $c \leftarrow c + 1$;
25 **until** $\kappa^{(c)} = \kappa^{(c-1)}$;
26 $\kappa^* \leftarrow \kappa^{(c)}$; $\mu^* \leftarrow \mu$; $\alpha^* \leftarrow \alpha$;

The input of Algorithm 1 consists of an initial RRH-UE association $\kappa^{(0)}$, a set $\mathcal{S}$ ($\mathcal{S} \subseteq \mathcal{J}$) of UEs for demand scaling, and a positive value ϵ that is the tolerance of convergence. For the output, Algorithm 1 gives the optimized RRH-UE association κ^*, the corresponding optimal resource allocation μ^*, and the demand scaling factor α^*. The algorithm goes through all the candidate RRH-UE pairs for CoMP. For each candidate RRH-UE pair, the algorithm applies the partial optimality condition in Lemma 7. Specifically, if the condition in Line 12 is satisfied for any RRH-UE pair (i, j), then adding a CoMP link (i, j) improves the load levels. When the loop in Lines 6–15 ends, the newly optimized association

$\kappa^{(c)}$ is obtained. The computational method in Theorem 5 is implemented in Lines 16–21, by which we obtain the optimal demand scaling for the set $\mathcal{S}$ and the corresponding resource allocation to satisfy the scaled demands under $\kappa^{(c)}$.

The complexity of Algorithm 1 is analyzed as follows. For simplicity, we assume the operations on vectors are atomic and can be done in $O(1)$. By [41] (along with our proof for Theorem 5), the iterations in Lines 6–15 and Lines 17–21 have linear convergence such that the complexity of the two loops (i.e. the required number of iterations) with tolerance ϵ is $O(\log \frac{1}{\epsilon})$ [42, Page 37]. Besides, the outer for-loop runs in $O(mn)$, and is executed with a maximum of $m \times n$ times[2]. Hence the total complexity is $O(m^2 n^2 \log \frac{1}{\epsilon})$. We remark that our algorithm is scalable from the computational theory perspective, since it is polynomial in the number of RRHs and UEs. The tolerance parameter ϵ can be selected in an on-demand manner: the smaller the value of ϵ, the higher the accuracy of the algorithm, meanwhile requiring more iterations. Numerically, the impact of the tolerance parameter ϵ on the algorithm convergence is discussed later in Section V-E.

E. Priority-aware Per-user Rate Optimization

We show in this subsection how Algorithm 1 applies to optimizing per-user rate by taking into account priority. For the sake of presentation, we impose $\mathcal{K}$ to be an ordered set consisting of candidate UEs for rate enhancement. The UEs in $\mathcal{K}$ are arranged in descending order according to their priority. Without loss of generality, suppose $\mathcal{K} = \{1, 2, \ldots K\}$. For each UE k in $\mathcal{K}$, we assign a budget Δ_k for resource allocation. That is, Δ_k is the affordable increase of the maximum RRH load level for enhancing the rate of UE k. Denote by $\bar{\rho}_0$ the maximum RRH load level initially.

The optimization procedure is as follows. We first run Algorithm 1 with $\bar{\rho} = \bar{\rho}_0 + \Delta_1$ and $\mathcal{S} = \{1\}$. At convergence, the maximum load of RRHs equals Δ_1, and the rate of UE 1 after optimization is $\alpha^* d_1$. We then replace the original base demand d_1 by $\alpha^* d_1$ for UE 1, and run Algorithm 1 with $\bar{\rho} = \bar{\rho}_0 + \Delta_1 + \Delta_2$ and $\mathcal{S} = \{2\}$ for UE 2, and so on. The process repeats until we reach UE K. At the end, the delivered demand of all UEs in $\mathcal{K}$ would be enhanced, with the maximum RRH load being $\bar{\rho} = \rho_0 + \sum_{k \in \mathcal{K}} \Delta_k$.

F. Upper Bound for MaxD under Two Extra Constraints

We derive an upper bound for *MaxD* under two extra constraints on CoMP selection. Denote by $\mathcal{J}_i^+$ the RRH i's candidate set of served UEs, i.e., the set of UEs that may potentially be served by RRH i. The first constraint is as follows.

$$\text{Candidate UE constraints: } \kappa_{ij} = 0 \text{ if } j \notin \mathcal{J}_i^+, i \in \mathcal{I}. \quad (24)$$

We impose that for each UE, there is a dominant RRH (e.g. the one with the strongest signal or with the shortest distance to the UE etc.) that serves the UE all the time. We call this dominant RRH the home RRH. Denote by $\mathcal{J}_i^-$ the set of UEs

of which the home RRH is i. The second constraint is below.

$$\text{Candidate RRH constraints: } \kappa_{ij} = 1 \text{ if } j \in \mathcal{J}_i^-, i \in \mathcal{I}. \quad (25)$$

Define a matrix $\check{\kappa}$, where for any RRH i ($i \in \mathcal{R}$) entry $\check{\kappa}_{ij} = 1$ if $j \in \mathcal{J}_i^+$. Consider the optimization problem below.

$$\max_{\alpha > 0, \mu \geqslant 0} \quad \alpha \quad (26a)$$
$$\text{s.t.} \quad \mu_j \geqslant \alpha f_j(\mu, \check{\kappa}) \quad j \in \mathcal{S} \quad (26b)$$
$$\mu_j \geqslant f_j(\mu, \check{\kappa}) \quad j \in \mathcal{J} \backslash \mathcal{S} \quad (26c)$$
$$\sum_{j \in \mathcal{J}_i^-} \mu_j \leqslant \bar{\rho} \quad i \in \mathcal{R} \quad (26d)$$

Theorem 8. *Solving* (26) *yields an upper bound of* α *for MaxD with constraints* (24) *and* (25).

Proof. The proof is based on [30, Lemma 12]. The derivation below is under under constraints (24) and (25). By [30, Lemma 12], we conclude that for any CoMP selection κ, we always have $f_j(\mu, \kappa) \geqslant f_j(\mu, \check{\kappa})$ for any $\mu \geqslant 0$. In addition, $\sum_{j \in \mathcal{J}_i^-} \mu_j \leqslant \sum_{j \in \mathcal{J}_i} \mu_j$ holds for any $\mu \geqslant 0$ and any κ (note that $\mathcal{J}_i$ is related to κ). Therefore, (26) is indeed a relaxation of *MaxD* (with (24) and (25)), such that solving the former always yields a better (or at least no worse) objective function value than the latter at optimum. Hence the conclusion. $\square$

We remark that the upper bound is derived for *MaxD* under the two extra constraints (24) and (25), though not proved theoretically to be an exact upper bound of the original problem *MaxD*. On the other hand, with the two constraints, solving (26) for obtaining the bound is quite straightforward and computationally efficient.

We also remark that, for any specific UE j, letting $\mathcal{S} = \{j\}$ and solving the corresponding formulation (26) yield the upper bound of the satisfiable demand of UE j. In addition, denote by $\mathbf{d}_\mathcal{S}$ the demands of $\mathcal{S}$ before scaling. Then $|\mathcal{S}|$ is an upper bound for the number of users with demands being no less than $\alpha^* \mathbf{d}_\mathcal{S}$, under the worst channel conditions of $\mathcal{S}$.

V. SIMULATION

The C-RAN under consideration consists of one hexagonal region, within which multiple UEs and RRHs are randomly deployed. The RRHs are coordinated by the cloud and cooperate with each other for CoMP transmission. Initially, no UE is in CoMP, and each UE is served by the RRH with the best signal power. The network layout is illustrated in Figure 1. Parameter settings are given in Table I. The user demands setting is configured for doing performance benchmarking for the cases with high RRH loads. In our simulation, the user demand subject to scaling is initially uniform. We use the non-CoMP case as the baseline. In the non-CoMP case, each UE is served with its single RRH that is the home RRH. The user demand is set such that for the baseline, with $\alpha = 1.0$, there is at least one RRH i ($i \in \mathcal{R}$) reaching the load limit

---

[2]Because there are at most $m \times n$ links that can be added.

($\rho_i = \bar{\rho}$). This demand[3] is normalized by $M \times B$. For clarity, we let $\mathcal{J}_{(CoMP)}$ denote the set of CoMP UEs in the solution obtained from Algorithm 1. The performance is studied by using four metrics for evaluation, defined below, referred to as Metric 1), Metric 2), Metric 3), and Metric 4), respectively.

TABLE I
SIMULATION PARAMETERS.

Parameter	Value
Hexagon radius	$\{500, 100\}$ m
Carrier frequency	2 GHz
Total bandwidth	20 MHz
Number of UEs ($|\mathcal{J}|$)	$\{100, 570\}$
Number of RRHs ($|\mathcal{R}|$)	$\{10, 57\}$
Path loss	COST-231-HATA
Shadowing (Log-normal)	3 dB standard deviation
Fading	Rayleigh flat fading
Noise power spectral density	-173 dBm/Hz
RB bandwidth	180 KHz
Transmit power on one RB	400 mW
User demand distribution	Uniform
Convergence tolerance (ϵ)	10^{-4}
Demand scaling proportion ($|\mathcal{S}|/|\mathcal{J}|$)	$\{10, 20, 40, 60, 80, 100\}$ (%)

1) *Improvement of* α: The metric is the objective function of *MaxD*. It reflects the capacity improvement of $\mathcal{S}$ (i.e. the user-centric performance).
2) $|\mathcal{J}_{((CoMP))}|$: This metric is the number of UEs involved in CoMP. It is used to relate the amount of CoMP to the capacity improvement.
3) *Increase (abbreviated as "inc") of delivered demand*: The metric is the amount of relative increase of the total delivered demand. It reflects the capacity improvement of $\mathcal{J}$, (i.e., the network-wise performance).
4) $|\mathcal{J}_{(CoMP)} \cap \mathcal{S}|$: This metric is the number of CoMP UEs inside $\mathcal{S}$. The metric is used for examining how CoMP for UEs inside $\mathcal{S}$ affects the demand scaling performance. One can also infer the number of CoMP UEs outside $\mathcal{S}$ by this metric together with Metric 2).

In the remaining parts of the section, we show the four metrics as functions of the number of UEs in $\mathcal{S}$ (i.e., $|\mathcal{S}|$), and the RRH load limit $\bar{\rho}$. Since our proposed algorithm employs a user-centric strategy for demand scaling, as for comparison, we refer to the strategy of scaling up demand for all UEs as a fairness-based strategy.

A. Performance with Respect to $|\mathcal{S}|$ (with $\bar{\rho} = 1.0$)

By observing Figure 2, as expected for Metric 1), one can achieve more improvement of α by CoMP when the size of $\mathcal{S}$ is smaller. The reason is very understandable: With the same amount of resource, enhancing the performance for a small group of UEs is generally easier than for a larger group. CoMP achieves considerable improvement of α, ranging from 13% to 28%.

---

[3]The method of obtaining this user demand is as follows. For any initialized d_j ($j \in \mathcal{J}$), applying Theorem 5 directly yields the corresponding demand scaling factor α, which leads to that at least one RRH i ($i \in \mathcal{R}$) reaching the load limit. Our expected user demand equals the initial demand multiplied by this α.

The user-centric performance benefits from CoMP through both direct and indirect effects. For explanation, we use Figure 1 as an illustration. Figure 1 shows some snapshots of our experiments, where the UEs and the RRHs are illustrated by dots and rectangles, respectively. The non-CoMP UEs in $\mathcal{S}$ are marked red. The CoMP UEs in $\mathcal{S}$ are marked green. The CoMP UEs in $\mathcal{J}\backslash\mathcal{S}$ are marked blue. The other UEs are in light gray. Basically, there are two ways for enhancing the capacity performance of $\mathcal{S}$: Using CoMP for UEs in $\mathcal{S}$ or UEs in $\mathcal{J}\backslash\mathcal{S}$. That the former generates benefits is apparent, since the spectrum efficiency would be increased for $\mathcal{S}$, which is a direct effect of using CoMP. As for the latter, since CoMP raises the RRH resource efficiency for serving UEs, using CoMP for $\mathcal{J}\backslash\mathcal{S}$ costs less resource than the non-CoMP case. As a result, there would be more available resource for scaling up the demand of UEs in $\mathcal{S}$. Furthermore, the reduction of an RRH load results in lower interference to the other RRHs, leading to an indirect effect for performance enhancement. On the other hand, we remark that not every UE benefits from being served by CoMP. In Figure 1, those UEs in light gray do not fulfill Lemma 7 in CoMP selection. Experimentally, forcing them to use CoMP leads to virtually no capacity improvement or even worse performance, due to that those UEs may only have one RRH being in good channel condition to them. Such UEs would not benefit from CoMP.

The number of UEs participating in CoMP has a strong influence on Metric 1). This is analyzed based on three observations as follows. As the first observation, the trends of Metric 1) and Metric 2) are very similar. Both metrics are influenced by the size of $\mathcal{S}$. For the second observation, by Metric 2), when the size of $\mathcal{S}$ is smaller, more UEs tend to be involved in CoMP, which is the reason why Metric 1) gets better when $|\mathcal{S}|$ becomes smaller. The third observation explains why more UEs would be involved in CoMP when $|\mathcal{S}|$ becomes smaller. Note that though $|\mathcal{J}_{(CoMP)}|$ increases with the decrease of $|\mathcal{S}|$, $|\mathcal{J}_{(CoMP)} \cap \mathcal{S}|$ however decreases with $|\mathcal{S}|$ (see Metric 2) and Metric 4)). It means that, with the decrease of $|\mathcal{S}|$, more UEs outside $\mathcal{S}$ and fewer UEs inside $\mathcal{S}$ would participate in CoMP. The former increases faster than the reduction of the latter. Recall that using CoMP for $\mathcal{S}$ and $\mathcal{J}\backslash\mathcal{S}$ leads to direct and indirect effects of benefits. We conclude that the two effects affect the performance of $\mathcal{S}$ to different extents with respect to the group size of $\mathcal{S}$. The reason is that, if we scale up demands for many UEs, due to the resulted intensive traffic, directly using CoMP to raise the spectrum efficiency for $\mathcal{S}$ is the most effective way for improving the performance of α. One can see by Metric 4) that the number of CoMP UEs in $\mathcal{S}$ increases with $|\mathcal{S}|$. Though the network still gains from the indirect effect of CoMP, the benefit is much more limited compared to the direct effect. On the other hand, when only a small proportion of UEs requires demand scaling (i.e. small $|\mathcal{S}|$), the gain from the direct effect is limited by the number of UEs in $\mathcal{S}$. In this case, it is more beneficial to focus on the other UEs (i.e. $\mathcal{J}\backslash\mathcal{S}$) of which the number is much higher than $|\mathcal{S}|$. As a consequence, the indirect effect of CoMP becomes dominating, i.e., reducing the RRH load with CoMP in order to alleviate the interference to $\mathcal{S}$ for increasing α. Algorithm 1 indeed seeks for a resource configuration that
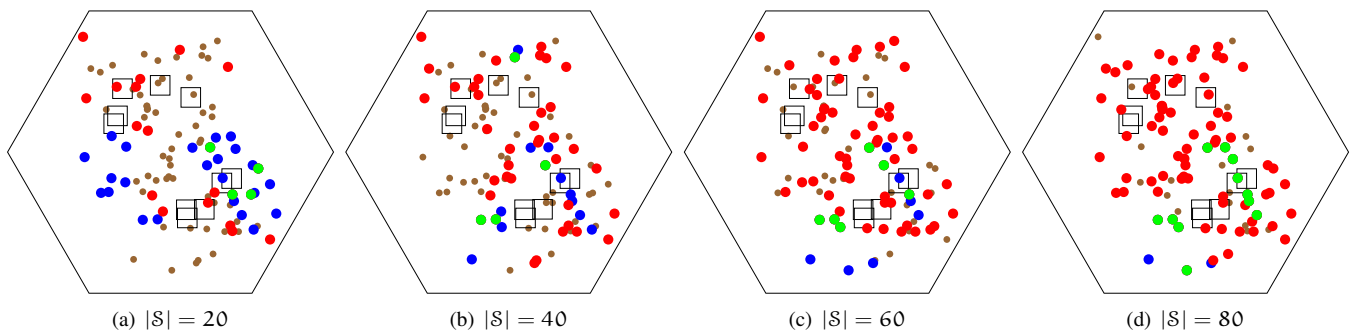
Figure 1. This figure shows some snapshots of the optimized CoMP selections. The UEs and the RRHs are illustrated by dots and rectangles, respectively. The number of UEs in $\mathcal{S}$ are 20, 40, 60, and 80, respectively. The non-CoMP UEs in $\mathcal{S}$ are marked red. The CoMP UEs in $\mathcal{S}$ are marked green. The CoMP UEs in $\mathcal{J}\setminus\mathcal{S}$ are marked blue. The other UEs are in brown. Note that the locations of RRHs are randomly generated within the hexagonal region in all our simulations. The figure is obtained from one simulation and is representative for all the simulation results.
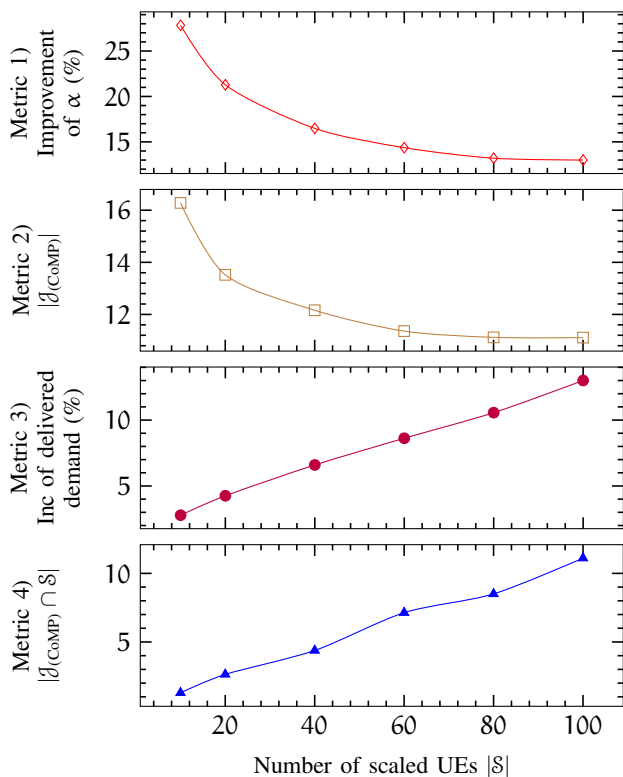
Figure 2. This figure shows the four metrics in function of $|\mathcal{S}|$. The non-CoMP case is used as baseline for Metrics 1) and 3).
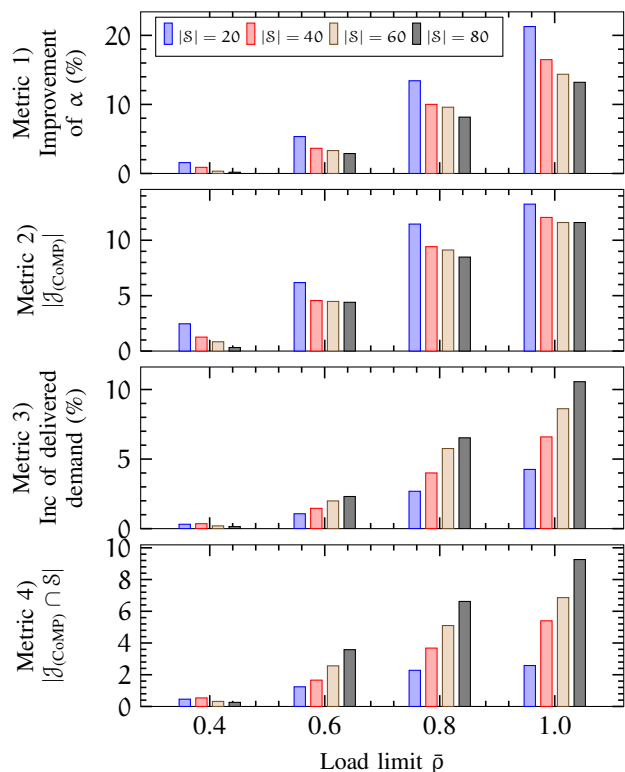

Figure 3. This figure shows the four metrics in function of $\bar{\rho}$. The non-CoMP case is baseline for Metrics 1) and 3). The legend applies to all subfigures.

maximumly leverages the two effects in order to achieve the highest improvement by CoMP. This is coherent with the snapshots in Figure 1. Visually, the ratio between CoMP UEs inside $\mathcal{S}$ over those outside $\mathcal{S}$ varies apparently with respect to $|\mathcal{S}|$.

In Figure 2, the user-centric capacity performance (i.e. Metric 1)) is different from the network-wise capacity performance (i.e. Metric 3)). Employing a user-centric strategy may help to deliver considerably more bits to those UEs to be scaled, compared to scaling up the demand for all UEs. If the group size is small, from the network's point of view, the capacity improvement is not as much as being achieved by scaling the demand for all UEs. Next, we observe that Metric 3) has a

strong correlation with Metric 4). The more UEs in $\mathcal{S}$ are served by CoMP, the more the bits can be delivered network-wisely. As one can see that though $|\mathcal{S}\cap\mathcal{J}_{(\text{CoMP})}|$ increases with respect to $\mathcal{S}$, $|\mathcal{J}_{(\text{CoMP})}| - |\mathcal{S}\cap\mathcal{J}_{(\text{CoMP})}|$ decreases (see this by combining Metric 4) with Metric 2)), meaning that the indirect effect of CoMP degenerates with $|\mathcal{S}|$ because the UEs outside $\mathcal{S}$ becomes fewer.

As a conclusion, user-centric demand scaling benefits from CoMP directly as well as indirectly. Namely, serving UEs inside $\mathcal{S}$ and outside $\mathcal{S}$ with CoMP both contribute.

B. Performance with Respect to $\bar{\rho}$

In Figure 3, we show Metrics 1)–4) as function of $\bar{\rho}$. As expected, the larger $\bar{\rho}$ is, the higher improvement can be achieved via CoMP. By both Metric 1) and Metric 3), when there is better availability of resource, the impact of the size of $\mathcal{S}$ on the achievable performance is higher. By Metric 3), one can see that the increase of total delivered demand is almost linear in $|\mathcal{S}|$ (when $\bar{\rho}$ is 0.6 or higher). Due to the limitation of resource availability when $\bar{\rho} = 0.4$, there may not be enough resource in RRHs for CoMP cooperations, even if we target scaling up demand for as many UEs as there are. As a consequence, the total delivered demand may not increase even if CoMP is enabled. One can see from Metric 2) that the number of UEs in CoMP is lower when $\bar{\rho} = 0.4$ than the cases with $\bar{\rho} \geqslant 0.6$. Specifically, the number of UEs in $\mathcal{S}$ that participate in CoMP is significantly lower when $\bar{\rho} = 0.4$, as shown by Metric 4). As another observation, one can see that Metric 3) and Metric 4) have the same trend under all settings of $\bar{\rho}$. It indicates that the direct effect of CoMP for UEs in $\mathcal{S}$ has a high correlation to the total delivered bits demand.

By combining Metric 2) with Metric 4), one can see that when $|\mathcal{S}|$ is small (e.g. $|\mathcal{S}| = 20$), though $|\mathcal{J}_{(\text{CoMP})}|$ increases quickly with $\bar{\rho}$, $|\mathcal{J}_{(\text{CoMP})} \cap \mathcal{S}|$ does slowly. It means that the number of CoMP UEs outside $\mathcal{S}$ increases quickly with the increase of the available resource. Hence, when there is more resource, it is more flexible for RRHs to cooperate in CoMP to serve $\mathcal{J}\backslash\mathcal{S}$ for RRH load reduction. As a consequence, the optimization leads to more UEs outside $\mathcal{S}$ to be involved in CoMP.

In conclusion, the availability of resource has an influence on the number of CoMP UEs. When $|\mathcal{S}|$ becomes smaller, the UEs in $\mathcal{S}$ benefit more from increasing $\bar{\rho}$ and more UEs outside $\mathcal{S}$ should be served by CoMP.

C. Performance with Respect to Resource Consumption

We show the relationship between user demand scaling/satisfaction and time-frequency resource allocation in Figure 4. Namely, we evaluate how much RRH load (i.e. amount of resource) is required to achieve more demand delivery by optimizing CoMP selection. Our test scenarios have 19 cells. The radius of each cell is 100 m. Each cell is deployed with 30 UEs and 3 RRHs. The other settings follow Table I.

Figure 4 compares the load levels of non-CoMP and CoMP, in order to show how much load is needed for achieving a 10%–15% increase of demand delivery by Algorithm 4. By observation, there is very slight difference in the total RRH load levels between non-CoMP and CoMP, though the latter delivers significantly more demand than the former. In addition, we found that optimizing the CoMP selection indeed reduces the average RRH load consumption for the highly-loaded RRHs. Therefore, we conclude that the time-frequency resource efficiency can be considerably improved by optimizing CoMP selection.

D. CoMP Selection Comparison

In this subsection, we compare our proposed CoMP selection mechanism with another one that is proposed for user-centric scenarios [43]. We tailor the CoMP selection method
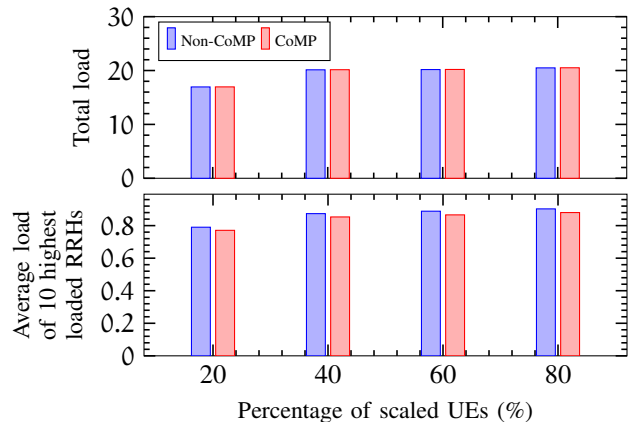

Figure 4. This figures shows the time-frequency resource consumption (i.e. RRH load) for delivering user demands. Though not shown by the figure, we remark that, with non-CoMP being the baseline, CoMP leads to 10%–15% percentage of improvement on α for all the data in this figure.

in [43] to be applicable in our model. We use the formula below as the utility of each UE for CoMP selection, which is designed for elastic application scenarios as considered by the authors.

$$u_j(C_j) = \frac{\ln(C_j + 1)}{\ln(d_j + 1)} \tag{27}$$

In (27), recall that C_j and d_j represent the achievable bits rate and the bits demand of UE j, respectively. Therefore we have $0 \leqslant u_j \leqslant 1$. Suppose κ is the current RRH-UE association, and κ' the a new association that differs with κ only in one RRH-UE pair (i, j) by $\kappa_{ij} = 0$ and $\kappa'_{ij} = 1$. By keeping the cell loads ρ fixed, we define the utility increase by adding the CoMP link (i, j) as $\Delta u_{ij} = u_j(C_j(\kappa')) - u_j(C_j(\kappa))$. The utility-based CoMP selection rule is: $\kappa_{ij} = 1$ if and only if $\Delta u_{ij} > 0$ $(i \in \mathcal{I}, j \in \mathcal{J})$. Once a new CoMP link is added, Theorem 5 is used to obtain the optimum of the remaining resource allocation problem. Therefore, the resource allocation is performed in the same manner for both our CoMP selection method and the utility-based one. The difference is that our method considers the interference influence caused by the dynamic change of RRH loads.

The comparison is shown in Figure 5. We can see that our proposed method outperforms the utility-based CoMP selection mechanism. In general, the improvement of α by our proposed CoMP seleciton is 1.5 times more than the utility-based CoMP selection. We remark that, compared to the utility-based CoMP selection, our proposed method takes into account the dynamic change of the cell load when a new CoMP link is added (see Section IV-C). Hence our proposed method outperforms the utility-based one, if cell load coupling is taken into account.

E. Convergence

We show by Figure 6 the convergence of the proposed method in (21) and (22), with $|\mathcal{S}| = 10, 40, 70, 100$. Initially we have $\alpha^{(0)} = 1$ and $\mu^{(0)} = 0$. Numerically, one can see that both α and μ converge fast. By Figure 6, under the same convergence tolerance parameter, the larger $|\mathcal{S}|$, the faster the
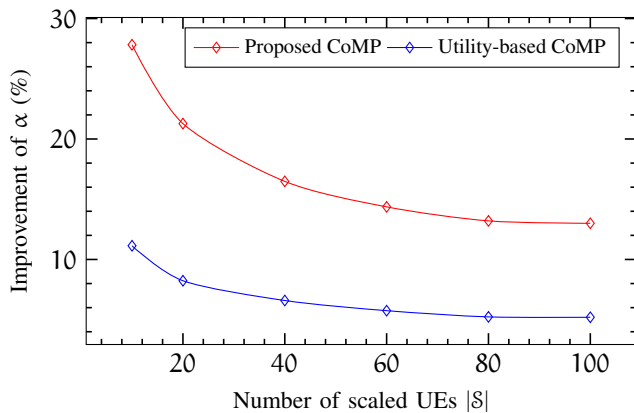
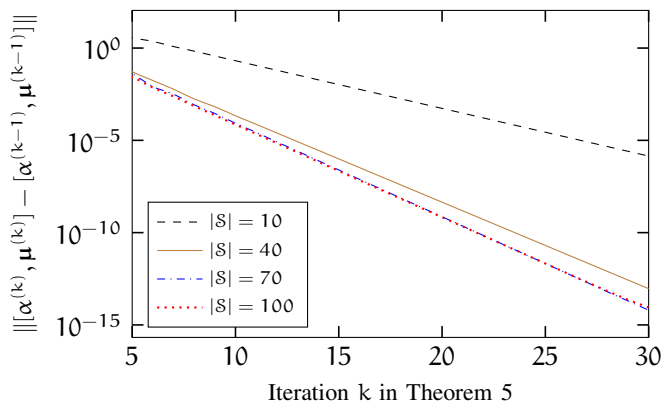Figure 5. Comparison of CoMP selection regarding the improvement of demand scaling.

Figure 6. This figures shows the norm $\|\cdot\|$ in function of iteration k in Theorem 5, under $|\mathcal{S}| = 10, 40, 70, 100$.

convergence. Moreover, larger $|\mathcal{S}|$ requires fewer algorithmic iterations, as it becomes fast for RRHs to reach the resource limit (i.e. the condition $H(\boldsymbol{\rho}) = 1$). As for our convergence tolerance setting $\epsilon = 10^{-4}$, the method converges within 25 iterations for all cases. We remark that when $|\mathcal{S}| = 100$, the iterations in Theorem 5 are actually computing the eigenvalue and eigenvector of a concave function and converge faster than the other cases. In general, Theorem 5 serves as an efficient sub-routine for Algorithm 1.

F. Additional Results with Presence of Fronthaul Capacity

In some scenarios, the capacity of the fronthaul links may turn out to be the performance bottleneck. Denote by the fronthaul link capacity limit of RRH i by c_i. Considering this capacity leads to the additional constraint of $\sum_{j \in \mathcal{J}_i \cap \mathcal{S}} \alpha d_j \leqslant c_i, i \in \mathcal{R}$.

Algorithm 1 can be easily extended to incorporate fronthaul capacity, by imposing a condition for Step 9. Namely, adding a link is considered, only if the capacity limit of the fronthaul of the RRH in question is not reached yet for the current demand scaling factor.

In Figure 7, we show the impact of fronthaul capacity on demand scaling. The maximum fronthaul capacity is set to a sufficiently large value such that it wouldn't be a bottleneck of
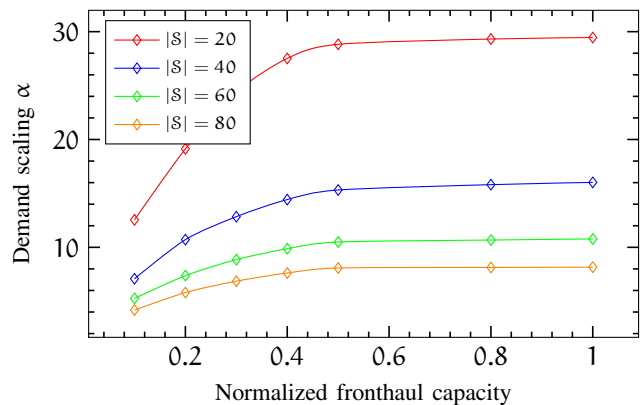

Figure 7. The impact of fronthaul capacity on demand scaling.

the system performance. The capacity shown in the x-axis is normalized with respect to this value. As can be seen, demand scaling is fronthaul-limited when the capacity is low, as increasing this capacity consistently improves the scaling factor. However, the curve becomes eventually saturated, meaning that the bottleneck is now due to radio access instead of the fronthaul. The results also show out algorithm is useful for studying which part of the network imposes the performance-limiting factor.

VI. CONCLUSION

We have proved how CoMP selection and demand scaling can be jointly optimized and demonstrated how CoMP improves the performance of user capacity in user-centric C-RAN. We have revealed that the users involved in demand scaling benefit both directly and indirectly from CoMP, by increasing the spectrum efficiency, and alleviating the interference among RRHs, respectively. Furthermore, the two effects contribute to the performance to different degrees with respect to the number of users for demand scaling. Finally, the user-centric demand scaling method proposed in this paper is not limited by the C-RAN architecture, and can be applied to other interference models that fall into the SIF framework.

One extension of the work is to consider beamforming by deploying multiple antennas at each RRH. This would bring additional performance gains, in addition to what the current work has focused on. As long as the strategy of setting the beamforming vector is given, our analysis remains applicable as the received signal and interference terms remain linear. On the other hand, joint optimization of association and beamforming, with presence of load coupling between the cells, leads to a new type of optimization problem for our forthcoming work.

APPENDIX
PROOF OF THEOREM 5

Lemma 9. *For any given $\alpha > 0$, denote $\boldsymbol{\mu}_\alpha = \lim_{k \to \infty} \boldsymbol{\mu}_\alpha^{(k)}$ where*

$$\boldsymbol{\mu}_\alpha^{(k+1)} = \frac{\mathbf{F}_\alpha(\boldsymbol{\mu}^{(k)})}{H \circ \mathbf{F}_\alpha(\boldsymbol{\mu}^{(k)})}. \tag{28}$$

Then $H(\boldsymbol{\mu}_\alpha) = 1$ and $\mathbf{F}_\alpha(\boldsymbol{\mu}_\alpha) = \lambda_\alpha \boldsymbol{\mu}_\alpha$ for unique $\lambda_\alpha > 0$.

Proof. The lemma follows from Theorem 1 in [38]. □

Lemma 10. *For any given* $\mu \geqslant 0$*, define* $P : \mathbb{R}_{++} \to \mathbb{R}_{++}$*:*

$$P : \alpha \mapsto \frac{1}{H \circ \mathbf{F}_\alpha(\mu)}. \qquad (29)$$

Then $P(\alpha)$ *is an SIF.*

Proof. Given μ, denote $\varphi_j = f_j(\mu)$. Then

$$P(\alpha) = \frac{1}{\frac{1}{\bar{\rho}} \max_{i \in \mathcal{R}} \sum_{j \in \mathcal{J}_i} \frac{\varphi_j}{\pi_j(\alpha)}}$$

For any $i \in \mathcal{R}$, the term $\sum_{j \in \mathcal{J}_i} \frac{\varphi_j}{\pi_j(\alpha)}$ is convex in α. Thus, the term $\max_{i \in \mathcal{R}} \sum_{j \in \mathcal{J}_i} \frac{\varphi_j}{\pi_j(\alpha)}$ is convex in α, and thus the function $P(\alpha)$ is concave in α (strictly concave if there is at least one j such that $\pi(\alpha) = \alpha$). The concavity implies the scalability. In addition, $P(\alpha)$ is monotonic in α. Hence the conclusion. □

Lemma 11. *For any* $\mu \in \mathbb{R}_+^n$ *and any* $\lambda \in \mathbb{R}_{++}$*,* $\lambda \geqslant \lambda_\alpha$ *if* $\lambda\mu \geqslant \mathbf{F}_\alpha(\mu)$*.*

Proof. The lemma follows from Theorem 13 in [38] . □

Lemma 12. *Define* $T : \mathbb{R}_{++} \to \mathbb{R}_{++}$*:*

$$T : \alpha \mapsto \frac{1}{H \circ \mathbf{F}_\alpha(\mu_\alpha)} \qquad (30)$$

where μ_α *follows the definition in Lemma 9. With* $\mathcal{S} \neq \phi$*,* $T(\alpha)$ *is an SIF.*

Proof. By Lemma 9, we have $\mathbf{F}_\alpha(\mu_\alpha) = \lambda_\alpha\mu_\alpha$. Thus, for function T, $T(\alpha) = 1/H(\lambda_\alpha\mu_\alpha)$ holds. Since $H(\mu_\alpha) = 1$, we have

$$T(\alpha) = 1/H \circ \mathbf{F}_\alpha(\mu_\alpha) = 1/\lambda_\alpha H(\mu_\alpha) = 1/\lambda_\alpha \qquad (31)$$

We first prove the monotonicity. Suppose $\alpha' > \alpha$. We use $\lambda_{\alpha'}$ and $\mu_{\alpha'}$ to represent respectively the eigenvalue and the eigenvector of $\mathbf{F}_{\alpha'}$ such that $\mathbf{F}_{\alpha'}(\mu') = \lambda_{\alpha'}\mu_{\alpha'}$ and $H(\mu_{\alpha'}) = 1$. For vector μ_α, one can easily verify that $\mathbf{F}_{\alpha'}(\mu_\alpha) \leqslant \mathbf{F}_\alpha(\mu_\alpha)$. Therefore $\lambda_\alpha\mu_\alpha \geqslant \mathbf{F}_{\alpha'}(\mu_\alpha)$. By Lemma 11, $\lambda_{\alpha'} \leqslant \lambda_\alpha$. Hence $T(\alpha') \geqslant T(\alpha)$ and the monotonicity holds.

We then prove the scalability. Consider for any $\eta > 1$ the function $\frac{1}{\eta}\mathbf{F}_\alpha(\mu)$, and denote by λ' and μ' respectively its eigenvalue and eigenvector, i.e., $\frac{1}{\eta}\mathbf{F}_\alpha(\mu') = \lambda'\mu'$. Denote by $\lambda_{\eta\alpha}$ and $\mu_{\eta\alpha}$ respectively the eigenvalue and eigenvector of function $\mathbf{F}_{\eta\alpha}$, i.e., $\mathbf{F}_{\eta\alpha}(\mu_{\eta\alpha}) = \lambda_{\eta\alpha}\mu_{\eta\alpha}$. For vector $\mu_{\eta\alpha}$, one can verify that the following relation holds.

$$\lambda_{\eta\alpha}\mu_{\eta\alpha} = \mathbf{F}_{\eta\alpha}(\mu_{\eta\alpha}) \geqslant \frac{1}{\eta}\mathbf{F}_\alpha(\mu_{\eta\alpha}) \qquad (32)$$

Based on Lemma 11, $\lambda' \leqslant \lambda_{\eta\alpha}$ holds. Specifically, with $\mathcal{S} \neq \phi$, we have for at least one $i \in \mathcal{R}$ such that $\pi_i(\alpha) = 1$. We conclude $\lambda' < \lambda_{\eta\alpha}$ due to the monotonicity of $\mathbf{F}_\alpha(\mu)$ in μ. In addition, by (28), we have the equation below.

$$\mu' = \lim_{k \to \infty} \frac{\frac{1}{\eta}\mathbf{F}_\alpha(\mu^{(k)})}{H \circ \frac{1}{\eta}\mathbf{F}_\alpha^k(\mu)} = \lim_{k \to \infty} \frac{\mathbf{F}_\alpha(\mu^{(k)})}{H \circ \mathbf{F}_\alpha(\mu^{(k)})} = \mu_\alpha \qquad (33)$$

Also, we have

$$\frac{1}{\eta}\mathbf{F}_\alpha(\mu') = \lambda'\mu' \Leftrightarrow \mathbf{F}_\alpha(\mu') = \eta\lambda'\mu'. \qquad (34)$$

Therefore, by Lemma 9, $\eta\lambda' = \lambda_\alpha$, i.e. $1/\lambda' = \eta/\lambda_\alpha$. Combined with $\lambda' < \lambda_{\eta\alpha}$, we have

$$T(\eta\alpha) = \frac{1}{\lambda_{\eta\alpha}} < \frac{1}{\lambda'} = \frac{\eta}{\lambda_\alpha} = \eta T(\alpha). \qquad (35)$$

Hence the conclusion. □

We then prove Theorem 5 as follows.

Proof. The proof is straightforward, based on Lemmas 9, Lemma 10, and Lemma 12. Denote by $\alpha_\mu^{(0)}, \alpha_\mu^{(1)}, \ldots, \alpha_\mu$ the sequence generated by $P(\alpha)$, with any $\alpha_\mu^{(0)} > 0$, for any given $\mu \geqslant 0$. By Lemma 10, α_μ is unique for μ. Similarly, denote by $\mu_\alpha^{(0)}, \mu_\alpha^{(1)}, \ldots, \mu_\alpha$ the sequence generated by (28), with any $\mu_\alpha^{(0)} \geqslant 0$, for any given $\alpha > 0$. By Lemma 9, α_μ is unique for α, and at the convergence we have $H(\mu_\alpha) = 1$. According to Lemma 12, $T(\alpha)$ is an SIF of α, then the α^* satisfying $\alpha^* = T(\alpha^*)$ is unique. By fixing one of α and μ and compute the sequence for the other alternately, the process falls into the category of asynchronous fixed point iterations, of which the convergence is guaranteed [44, Page 434]. At the convergence, we have some $\mu^* \geqslant 0$ such that

$$\mu^* = \frac{\mathbf{F}_\alpha^*(\mu^*)}{H \circ \mathbf{F}_\alpha^*(\mu^*)}, \text{ with } H(\mu^*) = 1. \qquad (36)$$

Hence the conclusion. □

PROOF OF THEOREM 6

Proof. The proof is based on the fact that the solution obtained from Theorem 5 fulfills Lemma 4. First, by Lemma 9, in the iterations in Theorem 5 we have $\mathbf{F}_{\alpha^*}(\mu^*) = \lambda_{\alpha^*}\mu^*$ for a unique $\lambda_{\alpha^*} > 0$ such that $H(\mu^*) = 1$. Also, $\alpha^* = 1/H\circ\mathbf{F}(\mu^*)$. Then, by combining these two equalities we get:

$$\alpha^* = \frac{1}{H(\lambda_{\alpha^*}\mu^*)} = \frac{1}{\lambda_{\alpha^*}H(\mu^*)}. \qquad (37)$$

Since $H(\mu^*) = 1$, we then have:

$$\lambda_{\alpha^*} = \frac{1}{\alpha^*}. \qquad (38)$$

Hence we obtain the following derivation:

$$\mathbf{F}_{\alpha^*}(\mu^*) = \frac{1}{\alpha^*}\mu^* \Leftrightarrow \alpha^*\mathbf{F}_{\alpha^*}(\mu^*) = \mu^* \Leftrightarrow$$
$$\frac{\alpha^* f_j(\mu)}{\pi_j(\alpha^*)} = \mu_j^* \quad j \in \mathcal{J} \Leftrightarrow \begin{cases} \mu_j = \alpha^* f_j(\mu^*) & j \in \mathcal{S} \\ \mu_j = f_j(\mu^*) & j \in \mathcal{J}\backslash\mathcal{S} \end{cases} \qquad (39)$$

By Lemma 4, i.e., the sufficient condition of optimality, the theorem hence holds. □

References

[1] L. You and D. Yuan, "Joint CoMP-cell selection and resource allocation with fronthaul-constrained C-RAN," in *2017 WiOpt Workshops*, 2017, pp. 1–6.

[2] "Cloud RAN - The benefits of virtualization, centralization and coordination," Ericsson, Tech. Rep., 2015.

[3] M. Peng, Y. Li, Z. Zhao, and C. Wang, "System architecture and key technologies for 5G heterogeneous cloud radio access networks," *IEEE Network*, vol. 29, no. 2, pp. 6–14, 2015.

[4] G. Liu, "5G-user centric network (Talk)," in *2015 Asia-Pacific Microwave Conference*, vol. 1, 2015, pp. 1–1.

[5] C. Pan, H. Zhu, N. J. Gomes, and J. Wang, "Joint precoding and RRH selection for user-centric green MIMO C-RAN," *IEEE Transactions on Wireless Communications*, vol. 16, no. 5, pp. 2891–2906, 2017.

[6] T. Hoßfeld, L. Skorin-Kapov, P. E. Heegaard, and M. Varela, "Definition of QoE fairness in shared systems," *IEEE Communications Letters*, vol. 21, no. 1, pp. 184–187, 2017.

[7] S. Chen, F. Qin, B. Hu, X. Li, and Z. Chen, "User-centric ultra-dense networks for 5G: Challenges, methodologies, and directions," *IEEE Wireless Communications*, vol. 23, no. 2, pp. 78–85, 2016.

[8] X. Xiao and L. M. Ni, "Internet QoS: A big picture," *The Magazine of Global Internetworking*, vol. 13, no. 2, pp. 8–18, 1999.

[9] "Vocabulary and effects of transmission parameters on customer opinion of transmission quality," ITU-T, Tech. Rep. Rec. P.10/G.100, Amendment 2, 2008.

[10] H. Zhang, C. Jiang, J. Cheng, and V. C. M. Leung, "Cooperative interference mitigation and handover management for heterogeneous cloud small cell networks," *IEEE Wireless Communications*, vol. 22, no. 3, pp. 92–99, 2015.

[11] A. Davydov, G. Morozov, I. Bolotin, and A. Papathanassiou, "Evaluation of joint transmission CoMP in C-RAN based LTE-A HetNets with large coordination areas," in *2014 IEEE Globecom Workshops*, 2014, pp. 801–806.

[12] A. Beylerian and T. Ohtsuki, "Multi-point fairness in resource allocation for C-RAN downlink CoMP transmission," *EURASIP Journal on Wireless Communications and Networking*, vol. 2016, no. 1, pp. 1–10, 2016.

[13] J. Ortín, J. R. Gállego, and M. Canales, "Joint cell selection and resource allocation games with backhaul constraints," *Pervasive and Mobile Computing*, vol. 35, pp. 125–145, 2017.

[14] A. Abdelnasser and E. Hossain, "Resource allocation for an OFDMA cloud-RAN of small cells underlaying a macrocell," *IEEE Transactions on Mobile Computing*, vol. 15, no. 11, pp. 2837–2850, 2016.

[15] W. Zhao and S. Wang, "Traffic density-based RRH selection for power saving in C-RAN," *IEEE Journal on Selected Areas in Communications*, vol. 34, no. 12, pp. 3157–3167, 2016.

[16] R. G. Stephen and R. Zhang, "Green OFDMA resource allocation in cache-enabled CRAN," in *2016 IEEE OnlineGreenComm*, 2016, pp. 70–75.

[17] R. G. Stephen and R. Zhang, "Fronthaul-limited uplink OFDMA in ultra-dense CRAN with hybrid decoding," *IEEE Transactions on Vehicular Technology*, vol. PP, no. 99, pp. 1–1, to appear.

[18] K. Wang, W. Zhou, and S. Mao, "On joint BBU/RRH resource allocation in heterogeneous cloud-RANs," *IEEE Internet of Things Journal*, vol. PP, no. 99, pp. 1–1, to appear.

[19] Y. L. Lee, L. C. Wang, T. C. Chuah, and J. Loo, "Joint resource allocation and user association for heterogeneous cloud radio access networks," in *2016 International Teletraffic Congress*, vol. 1, 2016, pp. 87–93.

[20] D. Mishra, P. C. Amogh, A. Ramamurthy, A. A. Franklin, and B. R. Tamma, "Load-aware dynamic RRH assignment in cloud radio access networks," in *2016 IEEE Wireless Communications and Networking Conference*, 2016, pp. 1–6.

[21] V. I. Tatsis, M. Karavolos, D. N. Skoutas, N. Nomikos, D. Vouyioukas, and C. Skianis, "Energy-aware clustering of CoMP-DPS transmission points," *Computer Communications*, vol. 135, pp. 28–39, 2019.

[22] M. Servetnyk and C. C. Fung, "Distributed joint transmitter design and selection using augmented admm," in *ICASSP 2019-2019 IEEE International Conference on Acoustics, Speech and Signal Processing (ICASSP)*. IEEE, 2019, pp. 4235–4239.

[23] M. S. Ali, E. Hossain, and D. I. Kim, "Coordinated multipoint transmission in downlink multi-cell multi-cell NOMA systems: Models and spectral efficiency performance," *IEEE Wireless Communications*, vol. 25, no. 2, pp. 24–31, 2018.

[24] Y. Luo, K. Yang, Q. Tang, J. Zhang, P. Li, and S. Qiu, "An optimal data service providing framework in cloud radio access network," *EURASIP Journal on Wireless Communications and Networking*, vol. 2016, no. 1, pp. 1–11, 2016.

[25] H. Ren, N. Liu, C. Pan, X. You, and L. Hanzo, "Power-and rate-adaptation improves the effective capacity of C-RAN for nakagami-m fading channels," *CoRR*, vol. abs/1704.01924, 2017. [Online]. Available: http://arxiv.org/abs/1704.01924

[26] K. Suto, K. Miyanabe, H. Nishiyama, N. Kato, H. Ujikawa, and K. I. Suzuki, "QoE-guaranteed and power-efficient network operation for cloud radio access network with power over fiber," *IEEE Transactions on Computational Social Systems*, vol. 2, no. 4, pp. 127–136, 2015.

[27] Z. Wang, D. W. K. Ng, V. W. S. Wong, and R. Schober, "Transmit beamforming for QoE improvement in C-RAN with mobile virtual network operators," in *2016 IEEE ICC*, 2016, pp. 1–6.

[28] A. J. Fehske, I. Viering, J. Voigt, C. Sartori, S. Redana, and G. P. Fettweis, "Small-cell self-organizing wireless networks," *Proceedings of the IEEE*, vol. 102, no. 3, pp. 334–350, 2014.

[29] I. Siomina and D. Yuan, "Analysis of cell load coupling for LTE network planning and optimization," *IEEE Transactions on Wireless Communications*, vol. 11, no. 6, pp. 2287–2297, 2012.

[30] L. You and D. Yuan, "Load optimization with user association in cooperative and load-coupled LTE networks," *IEEE Transactions on Wireless Communications*, vol. 16, no. 5, pp. 3218–3231, 2017.

[31] P. Mogensen, W. Na, I. Z. Kovacs, F. Frederiksen, A. Pokhariyal, K. I. Pedersen, T. Kolding, K. Hugl, and M. Kuusela, "LTE capacity compared to the Shannon bound," in *2007 IEEE VTC*, 2007, pp. 1234–1238.

[32] Q. Liao, D. Aziz, and S. Stanczak, "Dynamic joint uplink and downlink optimization for uplink and downlink decoupling-enabled 5g heterogeneous networks," *CoRR*, vol. abs/1607.05459, 2016. [Online]. Available: http://arxiv.org/abs/1607.05459

[33] I. Siomina and D. Yuan, "Optimizing small-cell range in heterogeneous and load-coupled LTE networks," *IEEE Transactions on Vehicular Technology*, vol. 64, no. 5, pp. 2169–2174, 2015.

[34] L. Ferdouse, A. Anpalagan, and S. Erkucuk, "Joint communication and computing resource allocation in 5g cloud radio access networks," *IEEE Transactions on Vehicular Technology*, 2019.

[35] I. Fajjari, N. Aitsaadi, and S. Amanou, "Optimized resource allocation and rrh attachment in experimental sdn based cloud-ran," in *Proc. of IEEE CCNC '19*, 2019.

[36] S. Ali, A. Ahmed, and A. Khan, "Energy-efficient resource allocation and rrh association in multitier 5g h-crans." *Transactions on Emerging Telecommunications Technologies*, 2019.

[37] G. Nigam, P. Minero, and M. Haenggi, "Coordinated multipoint joint transmission in heterogeneous networks," *IEEE Transactions on Communications*, vol. 62, no. 11, pp. 4134–4146, 2014.

[38] U. Krause, "Concave Perron–Frobenius theory and applications," *Nonlinear Analysis: Theory, Method & Applications*, vol. 47, no. 3, pp. 1457–1466, 2001.

[39] R. D. Yates, "A framework for uplink power control in cellular radio systems," *IEEE Journal on Selected Areas in Communications*, vol. 13, no. 7, pp. 1341–1347, 1995.

[40] L. You, L. Lei, and D. Yuan, "Load balancing via joint transmission in heterogeneous LTE: Modeling and computation," in *2015 IEEE PIMRC*, 2015, pp. 1173–1177.

[41] H. R. Feyzmahdavian, M. Johansson, and T. Charalambous, "Contractive interference functions and rates of convergence of distributed power control laws," *IEEE Transactions on Wireless Communications*, vol. 11, no. 12, pp. 4494–4502, 2012.

[42] Y. Nesterov, *Introductory Lectures on Convex Optimization: A Basic Course*. Springer Science & Business Media, 2013.

[43] A. Klockar, M. Sternad, A. Brunstrom, and R. Apelfröjd, "User-centric pre-selection and scheduling for coordinated multipoint systems," in *2014 11th International Symposium on Wireless Communications Systems (ISWCS)*, Aug 2014, pp. 888–894.

[44] D. P. Bertsekas and J. N. Tsitsiklis, *Parallel and Distributed Computation: Numerical Methods*. Prentice hall Englewood Cliffs, NJ, 1989.